SUPPLEMENTAL MATERIAL

SUPPLEMENTAL METHODS

Animals

Adult (10-12 weeks of age) male C57BL/6 mice (The Jackson Laboratory, Sacramento, CA, USA) were used for this study. All experimental procedures were approved by the Institutional Animal Care and Use Committee (IACUC) of Cedars-Sinai Medical Center and performed in accordance with National Institutes of Health guidelines.

Isoproterenol mini pump study

Fifty-six mice were randomized to receive a dose of 3×10^{10} vector genome (vg) of AAV9 transducing V5-tagged GFP or cBIN1 via retro-orbital injection while mice were anesthetized with 1% isoflurane in oxygen (1). Three weeks after viral injection, mice were subjected to implantation of osmotic mini pump releasing isoproterenol or PBS (N=14 per group for each of the four study groups: AAV9-GFP+PBS, AAV9-GFP+ISO, AAV9-cBIN1+PBS, AAV9-cBIN1+ISO). AAV9 was used in this study since AAV is the most promising gene therapy vehicle (2, 3) and AAV9 exhibits the highest cardiac tropism in mice (4-6). The CMV promoter was used since it has been established that AAV9-CMV can efficiently and safely direct cardiac gene transfer (7). AAV9-CMV-GFP was used as the negative control virus since AAV9-CMV-GFP does not induce cardiac damage and cardiomyocyte toxicity (7, 8), and GFP AAV9 has been successfully used as a negative control virus in numerous gene therapy studies with animal models of cardiovascular diseases, including mouse models of hypertrophy and cardiomyopathy (8-12).

This protocol was also repeated in a second set of animals. Similarly, three weeks before isoproterenol mini pump implantation, fifty mice were randomized to receive a dose of 3×10^{10} vector genome (vg) of AAV9 transducing V5-tagged GFP, BIN1, BIN1+13, BIN1+17, or cBIN1 (n=10 per group) via retro-orbital injection.

Three weeks after AAV9 injection, mice were implanted with subcutaneous ALZET osmotic mini pump (Model 1004, Durect, Cupertino, CA, USA) continuously releasing isoproterenol following previously established procedure (13). In brief, under light anesthesia with inhalation of

isoflurane, mice were implanted subcutaneously on the back with osmotic mini pumps, which continuously release isoproterenol at 30 mg/kg/day.

Generation and administration of adeno-associated virus 9 (AAV9)

All five AAV9 vectors expressing GFP-V5, BIN1-V5, BIN1+13-V5, BIN1+17-V5, and cBIN1-V5 (BIN1+13+17-V5) driven by the CMV promoter were custom made and produced at Welgen, Inc. (Worcester, MA, USA). We used previously reported gateway expression clones of V5-tagged GFP and mouse BIN1 isoforms (14), which were sequenced and then sent to Welgen for subsequent cloning into AAV vector and viral preparation. Next, these gene inserts (GFP-V5 or BIN1-V5) were subcloned into the pAAV-CMV vector (Welgen, Inc., Worcester, MA, USA), and the positive clones were selected by restriction enzyme digestion. The pAAV-CMV-(GFP/BIN1)-V5 plasmid DNA were purified and sequenced. All AAV viruses were produced in HEK293 cells. Three plasmids, pAAV-CMV-(GFP/BIN1)-V5, pAAV-rep/cap9, and pHelper vectors were transfected into 293 cells using polyethylenimine. Following transfection, the supernatant and cells were harvested. The AAV viruses were released from HEK293 cells by 3 freeze-thaw cycles. The viruses in the medium were precipitated using PEG8000 (Sigma-Aldrich, St. Louis, MO, USA). The cell lysate and pelleted supernatant precipitate were combined and treated by Benzonase (Merck, Kenilworth, NJ, USA) at 37°C for 1 h. The virus was purified by iodixanol gradient centrifugation and concentrated with Amicon Ultra-15 centrifugal filter (Sigma-Aldrich, St. Louis, MO, USA).

Transverse aortic constriction (TAC) study

For cBIN1 deficiency study, TAC was performed on male mice with cardiac-specific *Bin1* heterozygote deletion (*Bin1* HT; $Bin1^{flox/+}$, $Myh6\text{-}Cre^{+}$) and their wild type (WT; $Bin1^{flox/+}$, $Myh6\text{-}Cre^{-}$) littermates (WT) at the age of 8-10 weeks old (15). *Bin1* HT and WT mice were generated as previously described (15). Specifically, heterozygote loxp site flanked *Bin1* (loxP sites around exon 3 of the *Bin1* gene) mice were interbred with $Myh6\text{-}cre^{+}$ mice to generate cardiomyocyte specific *Bin1* HT (N=10) and WT littermate controls (n=14). Genotypes were confirmed by PCR to differentiate $Bin1^{+}$, $Bin1^{flox}$, and Cre^{+} alleles according to a previously established method1.

For AAV9 mediated over-expression study, 5 to 7-week old male C57BL/6J mice (Jackson Laboratory) received retro-orbital injection of AAV9 virus ($3x10^{10}$ vg) transducing cBIN1-V5 (N=18) or GFP-V5 (N=18). After three weeks, mice were anesthetized at the age of 8-10 weeks

and subjected to open-chest TAC surgery. Age-matched mice subjected to open-chest mock surgery without TAC being performed were used as sham controls (N=10).

TAC was performed to induce pressure overload as previously described. Briefly, 8-12 weeks old male mice were anesthetized by face mask administration of 3% isoflurane and then intubated and placed on a ventilator (Harvard Apparatus) with supplemental O2 and 1.5% isoflurane using a tidal volume of 0.2 ml and a respiratory rate of 120 breaths/min. The chest cavity was entered in the second intercostal space at the upper sternal border through a small incision, and aortic constriction was performed by tying a 7–0 nylon suture ligature against a 27-gauge needle between the first and second branch off the aortic arch. Subcutaneous buprenorphine (0.8 mg/kg) was administered for pain relief, and mice were allowed to recover in a heated chamber with 100% O2. Animals were euthanized, and tissues harvested for analysis after 8 weeks of TAC.

Echocardiographic evaluation

Cardiac dimensions and function in mice were assessed *in vivo* using a Vevo-3100 ultrasound system (Visual Sonics, Toronto, Canada) equipped with 70 MHz transducer. Briefly, mice were anesthetized with 5% isoflurane, shaved and placed in a supine position on a heating pad which maintained the body temperature at 37°C, then isoflurane was adjusted to about 2% to keep the heart rate 400-550 bpm and ECG was recorded. M-mode images in LV short axis view at the proximal level of papillary muscles were used for measurement of end-systolic and diastolic LV internal diameter (LVIDs/d), anterior wall thickness (AWT) and posterior wall thickness (PWT), as well as determination of LV mass (LVM) and relative wall thickness (RWT). Stroke volume (SV), cardiac output (CO), fractional area shortening (FS) and ejection fraction (EF) as well as left ventricular end-diastolic volume (LVEDV) and end-systolic volume (LVESV) were assessed from parasternal LV long axis view of two-dimensional image using LV trace method and were automatically calculated by the Vevo Lab software (Visual Sonics, Toronto, Canada). Each parameter was averaged from 3 to 5 cardiac cycles. In the TAC study, for comparison of effective aortic constriction between groups, the trans-aortic pressure gradient was recorded at 5 days post-surgery using the modified Bernoulli equation (Δ Pressure gradient (mmHg) = $4 * \text{peak velocity}^2$ $(\text{m/s})^2$.

In addition, LV diastolic function was assessed by Doppler echocardiography in apical four-chamber view. Transmitral flow velocity was evaluated by pulse-wave Doppler placing the

sample volume at the mitral leaflet tips. Wall velocity was evaluated by Tissue Doppler placing the sample volume at the septal mitral annulus. E/e' ratio (E, peak early transmitral blood flow velocity; e', the septal mitral annulus tissue velocity of early diastolic period) was calculated.

Western blot analysis

Frozen heart tissues were homogenized using RIPA lysis buffer with protease inhibitor, and a Bradford assay was used to determine the protein concentration (16). Samples were separated on NuPAGE™ Novex™ 4-12% Bis-Tris Protein Gels and then transferred to polyvinylidene difluoride membranes. After blocking for 1 h with 5% Bovine Serum Albumin (BSA) in 1xTNT buffer, membranes were incubated overnight at 4°C with primary antibody including rabbit anti GAPDH or Actin (Sigma-Aldrich, St. Louis, MO, USA), rabbit anti-$Ca_V1.2$ (Alomone Labs, Jerusalem, Israel), or mouse anti-SERCA2a (Abcam, Cambridge, MA, USA), followed by incubation with secondary antibody (goat anti rabbit or mouse IgG-Alexa 647) for 1.5 hour at room temperature (RT). Immunoreactive bands were imaged with the Molecular Imager® Gel Doc™ XR+ System (Bio-Rad Laboratories, Irvine, CA, USA) and band intensities quantified with Image Lab software (Bio-Rad Laboratories, Irvine, CA, USA).

Cardiac microsome preparation and sucrose gradient fractionation

Microsome sucrose gradient fractionation was prepared according to an established protocol with modifications (17). Myocardial membrane microsomes were prepared from starting material of one heart for each experimental group. Frozen heart tissue was homogenized with a Polytron Handheld homogenizer in 2 ml homogenization buffer (20 mM Tris pH 7.4, 250 mM sucrose, 1 mM EDTA supplemented with HALT protease inhibitor). The homogenate was then centrifuged at 12,000 g (Beckman) for 20 minutes at 4°C and the supernatant (S1) was collected in a pre-weighed tube and kept on ice. The pellet was resuspended in 1 ml of the same buffer, homogenized, and centrifuged at 12,000 g for 20 minutes at 4°C. The supernatant (S2) was collected and combined with the S1 from previous step. The combined microsomal supernatant (S1+S2) was then subjected to ultracentrifugation at 110,000 g for 2 hours at 4°C. After ultracentrifugation, the supernatant was disposed, the pellet was weighted, and the appropriate amount of buffer (~1 ml) was added to bring a final concentration of microsome ~25mg/ml. The total protein concentration in the resuspended microsome was measured using Nanodrop 2000 for each sample and normalized among the four groups. The same amount (3 - 6 mg in 0.5 ml) of total microsome from each sample was carefully laid over the top of a discontinuous sucrose gradient (27, 32, 38, and 45%, v/w in homogenization buffer, 2 ml each) and ultracentrifuged in

a fixed angle MLA-55 rotor at 150,000 g for 16 hours with a Beckman Coulter Optima Max XP Benchtop Ultracentrifuge. Samples were then collected from the following fractions: F1, 27%; F2, 27/32%; F3, 32/38%; and F4, 38/45%; as well as the pellet (P) from the bottom of the tube. For each fraction, ~1ml was collected, diluted 4x in homogenization buffer and ultracentrifuged at 120,000 g for 2 hours at 4°C. The pellet was resuspended in 100 μl of homogenization buffer, followed by protein concentration measurement by Nanodrop 2000. The yield of total amount of protein recovered from each fraction F1, F2, F3, F4 is between 0.001-0.02, 0.4-0.8, 0.04-0.06, and <0.008 mg per heart, respectively. Sample buffer was added before samples were frozen and stored at -20°C before subsequent Western Blot analysis.

Immunofluorescence labeling and imaging with spinning disc confocal microscopy

Myocardial tissue sections were embedded in 100% OCT media and flash frozen on dry ice with ethanol and stored in a -80°C freezer before being sectioned at 10 μm as previously reported (18). After fixation by acetone, tissue cryosections were permeabilized with 0.1% Triton X-100 and 5% normal goat serum (NGS, Life Technology) in PBS for 1 h at RT. For V5, $Ca_V1.2$, and SERCA2a staining, tissue sections were incubated with primary antibodies against rabbit anti-V5 (1:500, Sigma-Aldrich, St. Louis, MO, USA), rabbit anti-$Ca_V1.2$ (1:250, Alomone Labs, Jerusalem, Israel), or mouse anti-SERCA2a (1:250, Abcam, Cambridge, MA, USA) overnight at 4°C. After several washes with 1x PBS, tissue sections were then incubated with goat anti-mouse and anti-rabbit IgG conjugated with Alexa 488 and 555, respectively. Tissue sections were mounted with DAPI containing Prolong® Gold medium. All imaging was obtained with a Nikon Eclipse Ti microscope with a 40 × 1.1 or 100 × 1.49 numerical aperture total internal reflection fluorescence objective and NIS Elements software (Nikon, Los Angeles, CA, USA). Confocal Z stacks at Z-step increments of 0.5 μm were collected with a spinning-disk confocal unit (Yokogawa CSU10, Sugar Land, Texas, USA) connected to the same Ti microscope with diode-pumped solid state lasers (486, 561) generated from laser merge module 5 (Spectral Applied Research, Richmond Hill, Ontario, Canada), and captured by a high-resolution ORCA-Flash 4.0 digital CMOS camera. T-tubule Cav1.2 fluorescent intensity profiles were generated by ImageJ and peak intensity at t-tubules is quantified as previously reported (19). Calcium transients were performed following previously described protocol (20). Briefly, freshly isolated cardiomyocytes were loaded with 10 μmol/L Cal-520-AM (AAT Bioquest) in 0.4% Pluronic F-127 in normal Tyrode buffer for 30 minutes. After 3 washes in buffer containing 1mmol/L probenecid cells were placed in imaging chamber and paced with field stimulator (Ionflux) at 1 Hz. Images were collected using spinning disc confocal microscope at 67fps and analyzed using Nikon

Element Software. Fluorescent signals of F_0 (baseline fluorescence) and F_{max} (maximal fluorescence at the peak of calcium transient) were background corrected first followed by ratio calculation of $\Delta F/F_0 = (F_{max}-F_0)/F_0$ for comparison across groups.

Power Spectrum Analysis

The frequency domain power spectrum of cardiomyocyte immunofluorescent subsections was generated in Matlab using FFT conversion (19, 21). Power spectrum normalized to maximal component was generated and plotted over distance (1/frequency, μm). Normalized peak power density (22) was quantified and compared among groups.

Super-resolution Stochastic Optical Reconstruction Microscopy (STORM) Imaging and Nearest Neighbor Analysis

For STORM imaging, cardiomyocytes were prepared as previously reported (20). On the day of imaging, fresh STORM imaging buffer (0.5 mg/ml glucose oxidase, 40 μg/ml catalase, and 10% glucose with mercaptoethylamine) was added to the dish. The STORM images were collected with the Nikon Eclipse Ti microscope with lasers (488 561 from a self-contained 4-line laser module with acousto-optic tunable filters) and captured by a high-speed iXon DU897 Ultra EMCCD camera. The STORM module was used to obtained and analyze the images to generate 3-dimensional (3D) projections of Cav1.2/RyR and cBIN1/SERCA2a images at nanoscale resolution.

For nearest neighbor analysis, the native 3D STORM images are displayed with the gaussian rendering algorithm available in Nikon Elements software, and 3D stacks of 3D STORM images (two channels per acquisition, either Cav1.2/RyR or cBIN1/SERCA2a) in molecule list text file format were obtained at a z spacing of 10 nm for a depth of 500 nm. The molecule list text files were imported in ImageJ and the nearest distance between molecules from two channels (nearest neighbor distance) was calculated. The nearest neighbor distances were constructed and displayed in user-defined range and bin-width as frequency distribution histogram, and fitted in 15^{th}-degree polynomial curve with the first peak value detected. The distance between Cav1.2-RyR and SERCA2a-cBIN1 molecules at the corresponding first peak position were quantified and compared among groups.

Transmission Electron microscopy

All transmission electron microscopy (TEM) work was done by the core facility at the Electron Imaging Center of The California NanoSystems Institute, UCLA. Tissue preparation was performed using a previously reported method (23). Briefly, mouse hearts were perfused with 20 ml of fresh fixative solution (2% glutaraldehyde and 2% paraformaldehyde in 1x PBS). Left ventricular tissue (1 mm^3) were post-fixed with 1% osmium tetroxide and incubated in 3% uranyl acetate. After dehydration in ethanol, samples were treated with propylene oxide, embedded in Spurr resin (Electron Microscopy Services), and sectioned using an ultramicrotome (Leica). The sections were mounted on grid and stained with uranyl acetate and lead citrate before image acquisition using the JEM1200-EX, JEOL microscope (Gatan). The degree of contoured t-tubules was quantified using a modified scoring system established previously (15).

SUPPLEMENTAL REFERENCES

1. Basheer WA*, et al.* (2017) GJA1-20k Arranges Actin to Guide Cx43 Delivery to Cardiac Intercalated Discs. *Circ Res* 121(9):1069-1080.
2. Pacak CA & Byrne BJ (2011) AAV vectors for cardiac gene transfer: experimental tools and clinical opportunities. *Mol Ther* 19(9):1582-1590.
3. Skubis-Zegadlo J, Stachurska A, & Malecki M (2013) Vectrology of adeno-associated viruses (AAV). *Med Wieku Rozwoj* 17(3):202-206.
4. Inagaki K*, et al.* (2006) Robust systemic transduction with AAV9 vectors in mice: efficient global cardiac gene transfer superior to that of AAV8. *Mol Ther* 14(1):45-53.
5. Zincarelli C, Soltys S, Rengo G, & Rabinowitz JE (2008) Analysis of AAV serotypes 1-9 mediated gene expression and tropism in mice after systemic injection. *Mol Ther* 16(6):1073-1080.
6. Tilemann L, Ishikawa K, Weber T, & Hajjar RJ (2012) Gene therapy for heart failure. *Circ Res* 110(5):777-793.
7. Chen BD*, et al.* (2015) Targeting transgene to the heart and liver with AAV9 by different promoters. *Clin Exp Pharmacol Physiol* 42(10):1108-1117.
8. Chen Q*, et al.* (2017) Recombinant adeno-associated virus serotype 9 in a mouse model of atherosclerosis: Determination of the optimal expression time in vivo. *Mol Med Rep* 15(4):2090-2096.
9. Gallego-Colon E*, et al.* (2016) Intravenous delivery of adeno-associated virus 9-encoded IGF-1Ea propeptide improves post-infarct cardiac remodelling. *NPJ Regen Med* 1:16001.
10. Karakikes I*, et al.* (2013) Therapeutic cardiac-targeted delivery of miR-1 reverses pressure overload-induced cardiac hypertrophy and attenuates pathological remodeling. *J Am Heart Assoc* 2(2):e000078.
11. Denegri M*, et al.* (2014) Single delivery of an adeno-associated viral construct to transfer the CASQ2 gene to knock-in mice affected by catecholaminergic polymorphic ventricular tachycardia is able to cure the disease from birth to advanced age. *Circulation* 129(25):2673-2681.
12. Wang HL*, et al.* (2017) Prevention of Atrial Fibrillation by Using Sarcoplasmic Reticulum Calcium ATPase Pump Overexpression in a Rabbit Model of Rapid Atrial Pacing. *Med Sci Monit* 23:3952-3960.
13. Kudej RK*, et al.* (1997) Effects of chronic beta-adrenergic receptor stimulation in mice. *J Mol Cell Cardiol* 29(10):2735-2746.
14. Hong T*, et al.* (2014) Cardiac BIN1 folds T-tubule membrane, controlling ion flux and limiting arrhythmia. *Nat Med*.
15. Hong T*, et al.* (2014) Cardiac BIN1 folds T-tubule membrane, controlling ion flux and limiting arrhythmia. *Nat Med* 20(6):624-632.
16. Xu B*, et al.* (2017) The ESCRT-III pathway facilitates cardiomyocyte release of cBIN1-containing microparticles. *PLoS Biol* 15(8):e2002354.
17. Amoasii L*, et al.* (2013) Myotubularin and PtdIns3P remodel the sarcoplasmic reticulum in muscle in vivo. *J Cell Sci* 126(Pt 8):1806-1819.
18. Hong TT*, et al.* (2012) BIN1 is reduced and Cav1.2 trafficking is impaired in human failing cardiomyocytes. *Heart Rhythm* 9(5):812-820.
19. Hong TT*, et al.* (2010) BIN1 localizes the L-type calcium channel to cardiac T-tubules. *PLoS Biol* 8(2):e1000312.
20. Fu Y*, et al.* (2016) Isoproterenol Promotes Rapid Ryanodine Receptor Movement to Bridging Integrator 1 (BIN1)-Organized Dyads. *Circulation* 133(4):388-397.
21. Wei S*, et al.* (2010) T-tubule remodeling during transition from hypertrophy to heart failure. *Circ Res* 107(4):520-531.

22. Guo A & Song LS (2014) AutoTT: automated detection and analysis of T-tubule architecture in cardiomyocytes. *Biophys J* 106(12):2729-2736.
23. Basheer WA*, et al.* (2018) Stress response protein GJA1-20k promotes mitochondrial biogenesis, metabolic quiescence, and cardioprotection against ischemia/reperfusion injury. *JCI Insight* 3(20).

SUPPLEMETNAL FIGURE AND MOVIE LEGENDS

SUPPLEMENTAL FIGURE 1. (**A**) Representative fluorescent confocal images (20×) of V5 and WGA labeling in myocardial cryosections obtained from mice 7 weeks after injection of AAV9 transducing GFP-V5 or cBIN1-V5 or control hearts without AAV9 injection (negative control). Positive V5 signal is detected in 63% and 57% of cells from hearts 7 weeks after retro-orbital injection of AAV9-GFP-V5 or AAV9-cBIN1-V5 ($3x10^{10}$vg), respectively. Scale bar, 100 μm. (B) Quantitation of percent of myocardial area with detectable V5 signal. N=4-6 myocardial sections from 2-3 animals from each group. Data are presented as mean ± SEM. Kruskal-Wallis test was used followed by Dunns's test for multiple comparison. * indicates $p<0.05$ for vs no AAV9 negative control.

SUPPLEMENTAL FIGURE 2. (**A**) Echocardiography based categorization of LV remodeling in GFP+PBS, cBIN1+PBS, GFP+ISO, and cBIN1+ISO hearts. (**B**) Representative Western blot and quantification of α-smooth muscle actin in hearts from each group. Data are presented as mean ± SEM. Two-way ANOVA was used followed by Fisher's LSD test for multiple comparison. * indicates $p<0.05$ for PBS vs ISO comparison within each AAV9 treatment group; and $^{\#\#}$ indicates $p<0.01$ for GFP vs cBIN1 comparison within each drug infusion group.

SUPPLEMENTAL FIGURE 3. (**A**) Representative Western blot of total RyR_2 protein expressions in mouse with quantifications. (**B**) Representative confocal images (100×) of RyR_2 in mouse cardiomyocytes from each group followed by power spectrum analysis (n=33-36 cells from 3-4 hearts per group). Scale bar: 10 μm.

SUPPLEMENTAL FIGURE 4. Representative Western blots of RyR_2 (total and phosphorylated pS2814 and pS2808), Cav1.2, CAMKIIδ (total and phosphorylated pT287), and phospholamban (PLN, total and phosphorylated pS16 and pT17). Quantifications are included in the bar graphs to the right. Data are presented as mean ± SEM. N=4-7 hearts per group. Two-way ANOVA was used followed by Fisher's LSD test for multiple comparison. * indicates $p<0.05$ for PBS vs ISO comparison within each AAV9 treatment group; and $^{\#}$ indicates $p<0.05$ for GFP vs cBIN1 comparison within each drug infusion group.

SUPPLEMENTAL FIGURE 5. (**A**) Schematic protocol of sucrose gradient fractionation of cardiac microsomes (3-6 mg per heart). The yield of total amount protein recovered from each

fraction F1, F2, F3, F4 is between 0.001-0.02, 0.4-0.8, 0.04-0.06, and <0.008 mg per heart prep, respectively. (**B**) Representative Western blots of Cav1.2, Na^+/K^+-ATPase, SERCA2a, cBIN1, and caveolin 3 from the microsome input (M) and recovered fractions from F1, F2, F3, F4, and pellet from GFP+PBS, GFP+ISO, cBIN1+PBS, and cBIN1+ISO hearts.

SUPPLEMENTAL FIGURE 6. cBIN1 organizes LTCC and SERCA2a in post isoproterenol mouse hearts. **(A)** Representative Western blots of Cav1.2 and SERCA2a in post isoproterenol mouse hearts treated by AAV9-GFP, cBIN1, BIN1, BIN1+17, and BIN1+13. Quantification is included in the bar graphs to the right (n=3 hearts per group). Representative confocal images (100×) of anti-Cav1.2 (**B**) and anti-SERCA2a (**C**) labeling in mouse myocardium from each group. Scale bar: 5 μm. (**D**) Quantification of t-tubule Cav1.2 fluorescent intensity from each group. N=16-22 cells from 3 hearts from each group. (**E**) Quantification of SERCA2a peak power density from each group. N=20 cell images from 2-3 hearts from each group. Data are expressed as mean ± SEM. One-way ANOVA was used followed by Fisher's LSD test for multiple comparison. *, **, ***, indicate p<0.05, 0.01, 0.001 when compared to control GFP group.

SUPPLEMENTAL VIDEO 1. Representative three-dimensional (3D) STORM images of Cav1.2 (red) / RyR (green) couplons in cardiomyocytes isolated from GFP+PBS (**A**), cBIN1+PBS (**B**), GFP+ISO (**C**), or cBIN1+ISO (**D**) hearts.

SUPPLEMENTAL VIDEO 2. Representative three-dimensional (3D) STORM images of SERCA2a (green) / cBIN1 (red) couplons in cardiomyocytes isolated from GFP+PBS (**A**), cBIN1+PBS (**B**), GFP+ISO (**C**), or cBIN1+ISO (**D**) hearts.

SUPPLEMENTAL TABLE 1. Echocardiographic Parameters of AAV9-GFP or cBIN1 Injected Mice After 4 Weeks of PBS or ISO Infusion

	GFP+PBS (n=14)	**cBIN1+PBS** (n=14)	**GFP+ISO** (n=14)	**cBIN1+ISO** (n=14)
HW/BW (mg/g)	6.07± 0.15	5.65± 0.17	6.90± 0.18**	6.52± 0.20**
LVM (mg)	116.87± 4.71	119.19± 5.37	161.18± 5.45***	140.70± 3.33**##
RWT	0.35±0.02	0.38±0.02	0.58±0.04***	0.39±0.01###
LVEDV (µL)	49.11±2.15	47.70±2.48	41.58±3.06	57.21±3.06*##
SV (µL)	27.64±1.24	25.81±1.56	25.13±1.50	36.37±1.86***###
CO (mL/min)	12.70±0.58	12.32±0.67	14.68±0.90	20.95±0.99***###
HR (bpm)	454.41±10.90	481.30±13.70	583.41±9.87***	569.05±7.10***
EF (%)	56.43±1.31	54.19±1.68	61.98±2.65 (*p*=0.05 vs. GFP+PBS)	64.63±1.94***
E/e'	33.85±1.87	33.27±2.13	46.06±3.31**	34.51±2.44##

LVM, left ventricular mass; RWT, relative wall thickness; LVEDV, left ventricular end-diastolic volume; SV, stroke volume; CO, cardiac output; HR, heart rate; EF, ejection fraction; FS, fraction area shortening; E/e', transmitral blood flow velocity of early diastolic period/the septal mitral annulus tissue velocity of early diastolic period.

Data are expressed as Mean ± SEM. *, **, *** indicates *P*<0.05, 0.01, 0.001 respectively for comparison of PBS vs. ISO with the same AAV9 treatment; #, ##, ### indicates *P*<0.05, 0.01, 0.001 respectively for comparison of AAV8-GFP vs. AAV9-cBIN1 with isoproterenol (ISO) infusion.

SUPPLEMENTAL TABLE 2. Echocardiographic Parameters of AAV9-GFP or BIN1 isoforms-Injected Mice Before and After ISO Infusion

	Baseline					Pre-ISO					4w post-ISO				
	GFP	cBIN1	BIN1	BIN1+13	BIN1+17	GFP	cBIN1	BIN1	BIN1+13	BIN1+17	GFP	cBIN1	BIN1	BIN1+13	BIN1+17
LVM (mg)	116.49± 9.80	113.33± 5.70	115.52± 6.57	101.51± 4.38	96.78±5.38	106.55± 5.28	114.35± 4.48	113.69± 6.36	113.96± 4.05	106.66± 3.59	179.82± 16.14***	143.67± 6.92*##	162.89± 10.92***	152.89± 8.43***	142.87± 8.20***##
RWT	0.36±0.02	0.34±0.02	0.34±0.01	0.34±0.02	0.33±0.01	0.33±0.02	0.36±0.02	0.32±0.01	0.33±0.02	0.32±0.01	0.49±0.02***	0.41±0.02*##	0.48±0.03***	0.46±0.03***	0.45±0.02***
LVEDV (μL)	56.67±4.39	55.96±4.38	57.54±1.94	55.45±2.02	54.63±3.32	57.38±2.98	55.92±2.73	54.45±2.43	54.21±2.63	51.18±2.34	54.76±4.95	61.34±4.34	55.19±3.47	51.81±3.28	53.04±2.51
SV (μL)	29.15±2.47	29.16±1.95	30.49±1.38	29.33±1.43	28.69±1.85	29.04±1.75	29.03±1.70	28.92±1.39	29.53±1.57	27.50±1.26	31.00±1.88	36.94±1.66**#	28.98±1.53	29.78±1.19	31.35±1.36
CO (mL/min)	12.67±1.03	12.63±0.95	13.77±0.38	12.77±0.75	13.18±1.05	13.04±0.98	14.19±0.90	14.06±0.92	14.07±1.08	12.53±0.72	16.95±1.31**	21.02±1.13***#	17.92±0.99**	18.33±0.73***	18.32±1.03***
HR (bpm)	443±19	443±12	484±7	471±12	449±12	446±15	488±12	484±15	472±17	455±14	546±25***	568±13***	572±23***	589±12***	582±11***
EF (%)	52.02±1.22	52.75±1.66	53.49±0.78	52.96±0.82	53.05±0.82	50.66±1.46	51.84±1.62	53.19±1.00	54.43±1.09	53.79±1.13	58.40±2.97**	62.95±2.44***	52.97±1.64#	57.71±1.53	57.93±1.33
FS (%)	17.01±0.80	16.49±1.60	18.70±1.17	17.53±1.13	18.18±1.05	17.53±1.28	18.48±1.58	19.48±0.89	17.39±1.90	17.17±1.60	18.30±1.46	20.95±1.58*	18.13±1.79	18.90±1.25	18.37±1.08
E/e'	35.14±2.21	32.53±1.89	34.83±3.07	34.88±2.32	31.88±3.11	37.23±3.12	34.07±2.75	32.73±3.00	34.12±3.88	36.96±2.19	45.33±3.20*	32.39±2.37##	39.06±2.97	36.07±2.47	32.33±2.28##

LV geometry and function were evaluated by echocardiography at baseline, before isoproterenol infusion (Pre-ISO) and 4 weeks post isoproterenol treatment (4w post-ISO). LVM, left ventricular mass; RWT, relative wall thickness; LVEDV, left ventricular end-diastolic volume; SV, stroke volume; CO, cardiac output; HR, heart rate; EF, ejection fraction; FS, fraction area shortening; E/e', transmitral blood flow velocity of early diastolic period/the septal mitral annulus tissue velocity of early diastolic period.

Data are expressed as Mean ± SEM. *, **, *** indicates *P*<0.05, 0.01, 0.001 vs. the baseline of each own group; #, ##, ### indicates *P*<0.05, 0.01, 0.001 vs. the GFP group of 4w post-ISO.

SUPPLEMENTAL TABLE 3. Phenotype Characteristics in All Mice 8 Weeks after Sham or TAC Surgery.

Parameter	**WT** (n=12)	***Bin1* HT** (n=8)	**Sham** (n=10)	**AAV9-GFP** (n=14)	**AAV9-cBIN1** (n=16)
Pressure Gradient (mmHg)	68.16±3.07	62.77±7.54	2.22±0.22	70.21±3.96*	71.94±3.35*
BW (g)	29.66±.47	26.41±.86*	29.66±0.48	29.89±0.48	30.48±0.50
HW (g)	0.26±0.02	0.32±0.03	0.16±0.01	0.27±0.01*	0.23±0.01*
LW (g)	0.24±0.02	0.32±0.04*	0.19±0.01	0.29±0.03*	0.21±0.01
HW/BW (mg/g)	8.10±0.51	12.07±1.22**	5.20±0.28	9.16±0.58*	7.41±0.32*
LW/BW (mg/g)	8.11±0.80	2.32±2.03*	6.27±0.28	10.19±1.10*	6.94±0.40#

Data are expressed as Mean ± SEM. * indicates $p<0.05$ vs. WT or Sham; # indicates $p<0.05$ for AAV9-GFP vs. AAV9-cBIN1.

BW: body weight; HW: heart weight; LW: lung weight.

SUPPLEMENTAL TABLE 4. Echocardiographic Parameters in All Mice 8 Weeks after Sham or TAC Surgery.

Parameter	WT (n=12)	*Bin1* HT (n=8)	Sham (n=10)	AAV9-GFP (n=14)	AAV9-cBIN1 (n=16)
HR (bpm)	515.70±14.65	516.9±14.56	511.84±18.22	550.31±9.73	552.32±14.19
EF (%)	42.54±2.59	27.50±3.15**	60.04±1.38	42.69±2.43*	50.36±1.91*#
FS (%)	21.20±1.48	12.96±1.65*	29.78±0.78	21.06±1.40*	25.44±1.16#
EDV (µl)	88.25±4.68	110.60±9.23*	63.35±4.06	89.54±5.30*	71.97±3.35#
ESV (µl)	51.96±4.49	81.15±9.74*	24.59±2.62	51.05±3.46*	35.89±2.26#
SV (µl)	36.30±1.99	29.47±2.31*	38.76±1.88	38.49±3.48	36.08±2.01
CO (ml/min)	18.24±1.11	15.53±1.16	19.08±0.76	20.77±2.01	19.29±0.92
LVAWd (mm)	1.04±0.06	0.97±0.06	0.83±0.05	1.16±0.05*	1.12±0.06*
LVAWs (mm)	1.36±0.07	1.24±0.07	1.16±0.04	1.42±0.05*	1.44±0.08*
LVIDd (mm)	4.50±0.09	4.87±0.16*	3.92±0.10	4.50±0.13*	4.13±0.10
LVIDs (mm)	3.60±0.12	4.36±0.17*	2.74±0.16	3.69±0.11*	3.14±0.09 #
LVPWd (mm)	1.16±0.07	1.10±0.11	0.78±0.04	1.14±0.03*	1.16±0.06*
LVPWs (mm)	1.48±0.08	1.24±0.11*	1.19±0.07	1.33±0.06	1.46±0.05*
LV Mass (mg)	222.63±13.75	239.87±18.98	117.39±7.00	254.48±16.81*	215.70±11.40*#
E/e' lateral	44.36±7.89	49.73±6.64	34.26±4.15	44.30±4.62	28.81±1.96#
E/e' septal	44.70±4.89	49.93±8.89	40.94±4.77	46.31±5.32	30.64±1.78#

Data are expressed as Mean ± SEM. * indicates $p<0.05$ vs. WT or Sham; # indicates $p<0.05$ for AAV9-GFP vs. AAV9-cBIN1.

HR: heart rate; EF: ejection fraction; FS: fractional shortening; EDV: end diastolic volume; ESV, end systolic volume; SV: stroke volume; CO, cardiac output; LVAWd / LVAWs: left ventricular anterior wall in diastole / systole; LVIDd / LVIDs: left ventricular internal diameter in diastole / systole; LVPWd / LVPWs: left ventricular posterior wall in diastole/systole; E/e' lateral: transmitral blood flow velocity of early diastolic period / the lateral mitral annulus tissue velocity of early diastolic period; E/e' septal: transmitral blood flow velocity of early diastolic period / the septal mitral annulus tissue velocity of early diastolic period

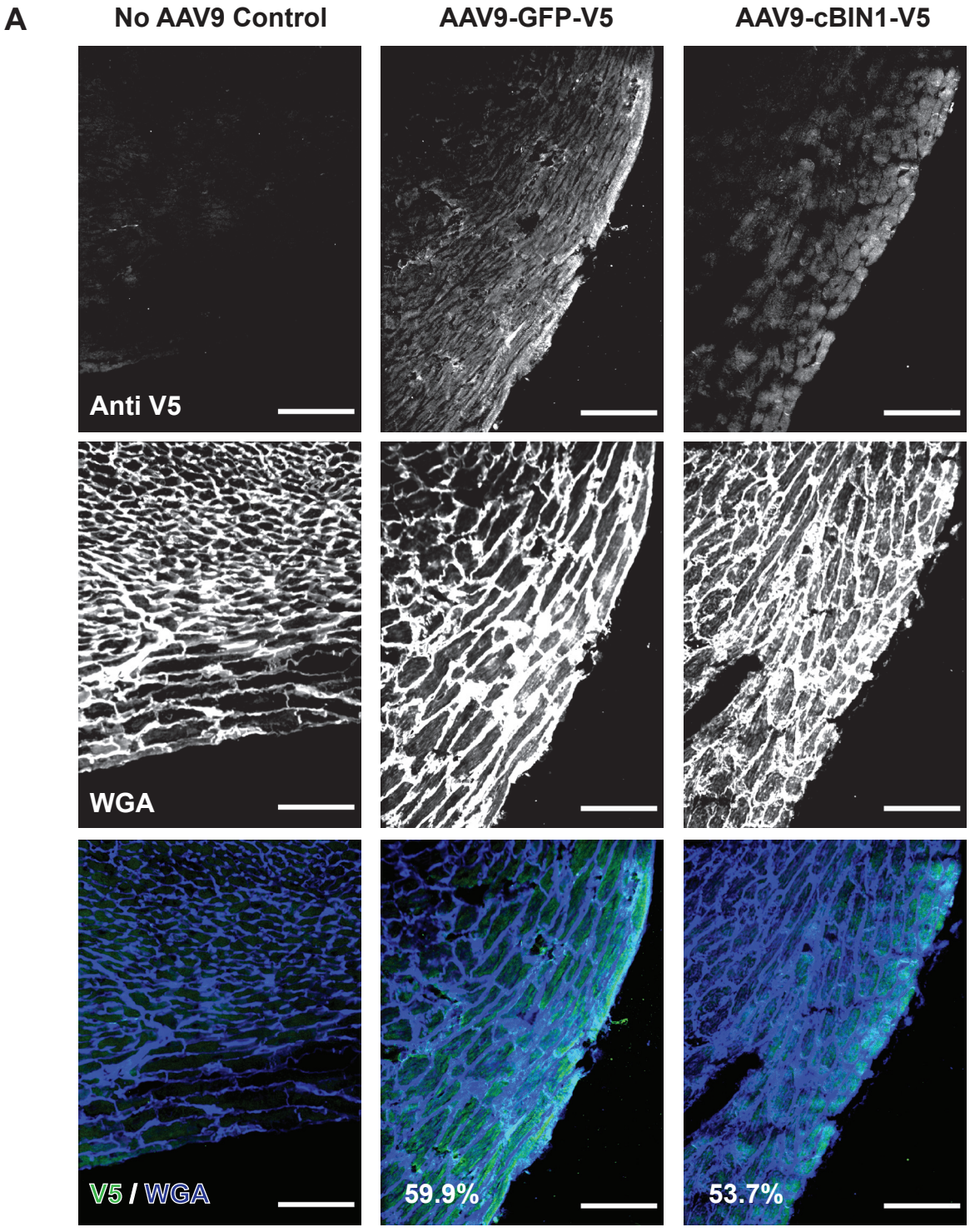

Supplemental Figure 1

A

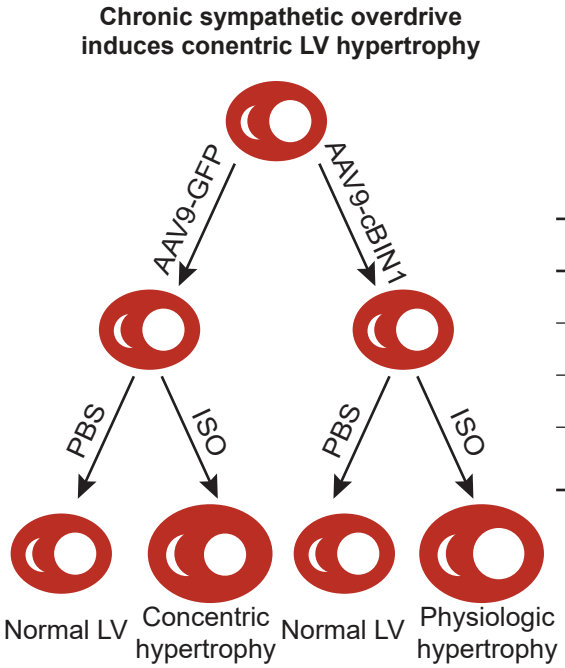

Pattens of LV Remodeling based on EDV, LV mass, and RWT

Treatment	EDV	LV Mass	RWT	Remodeling Pattern
GFP+PBS	—	—	—	Normal LV
cBIN1+PBS	—	—	—	Normal LV
GFP+ISO	—	↑	↑	Concentric hypertrophy
cBIN1+ISO	↑	↑	—	Physiologic hypertrophy

B

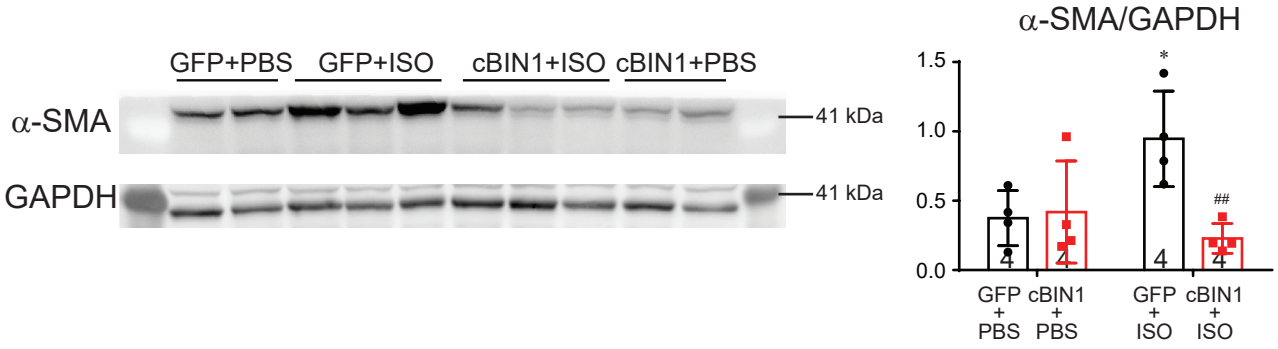

Supplemental Figure 2

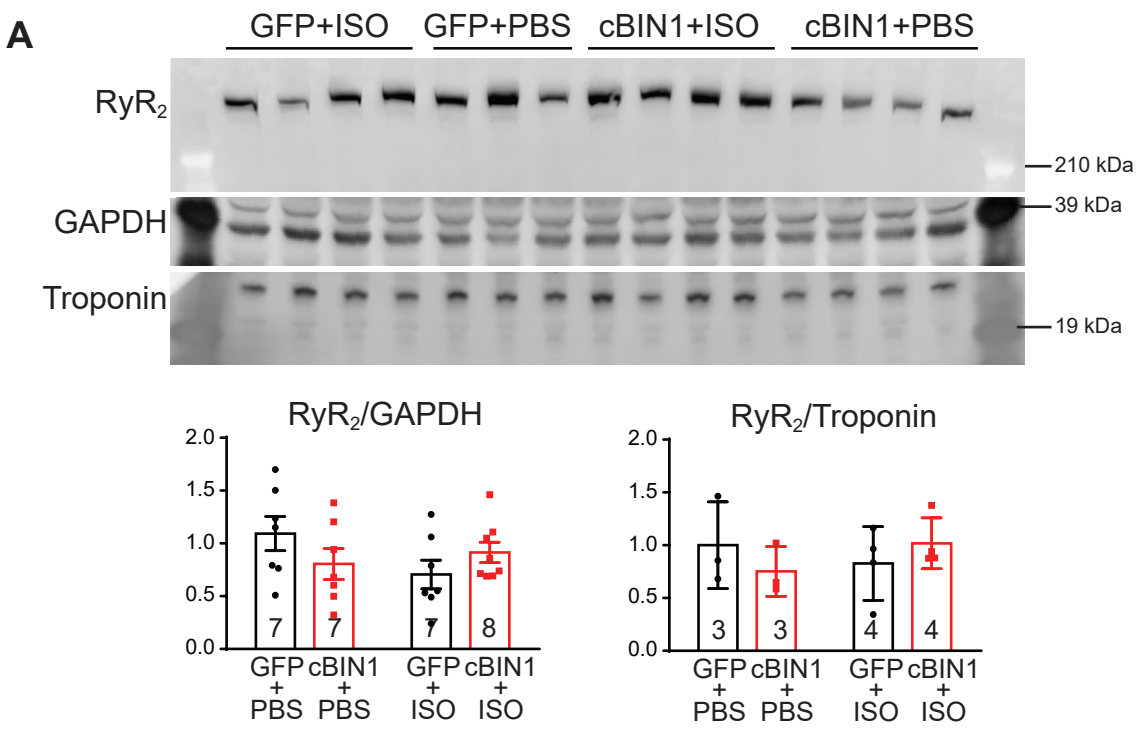

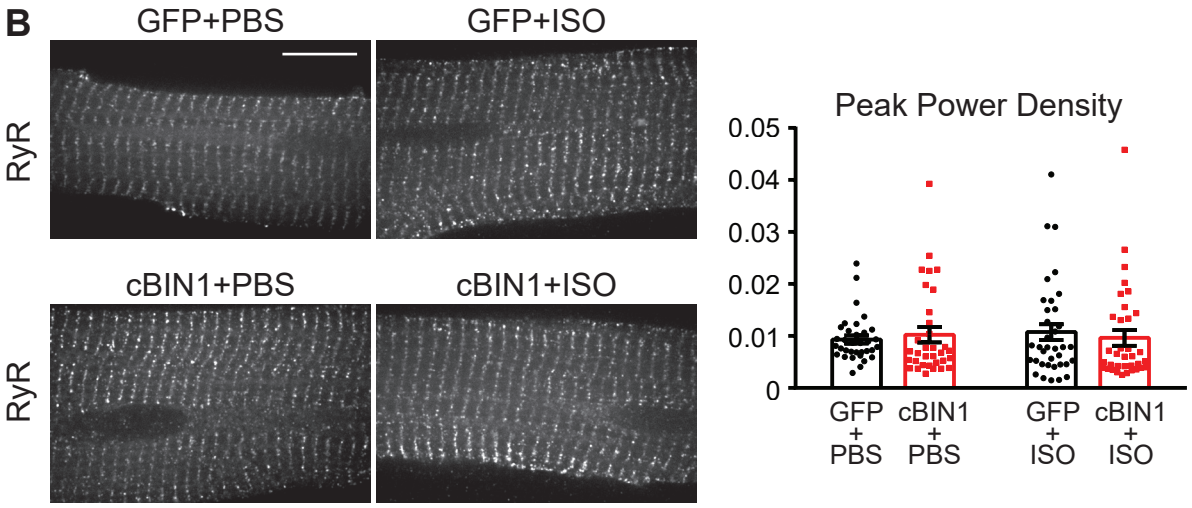

Supplemental Figure 3

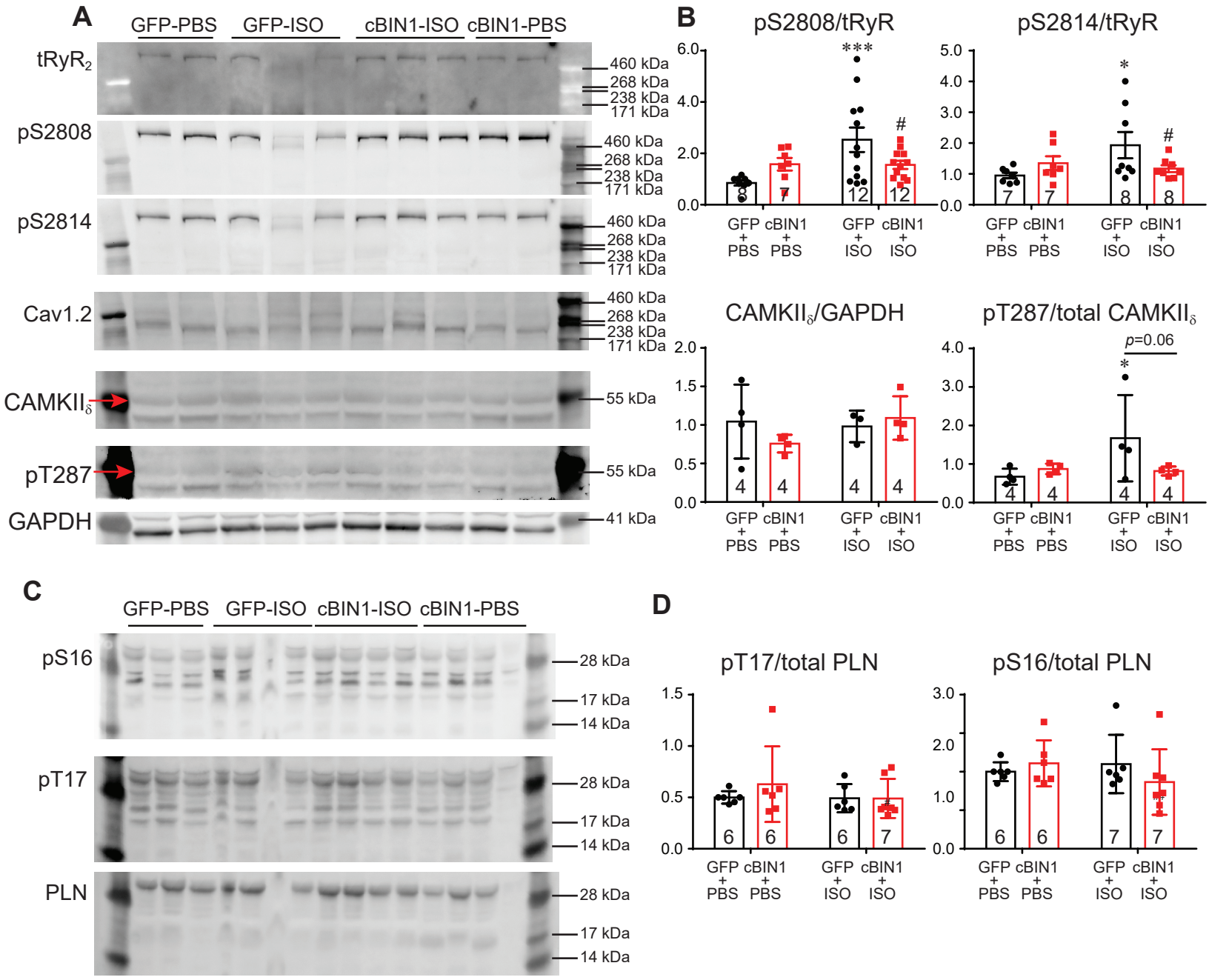

Supplemental Figure 4

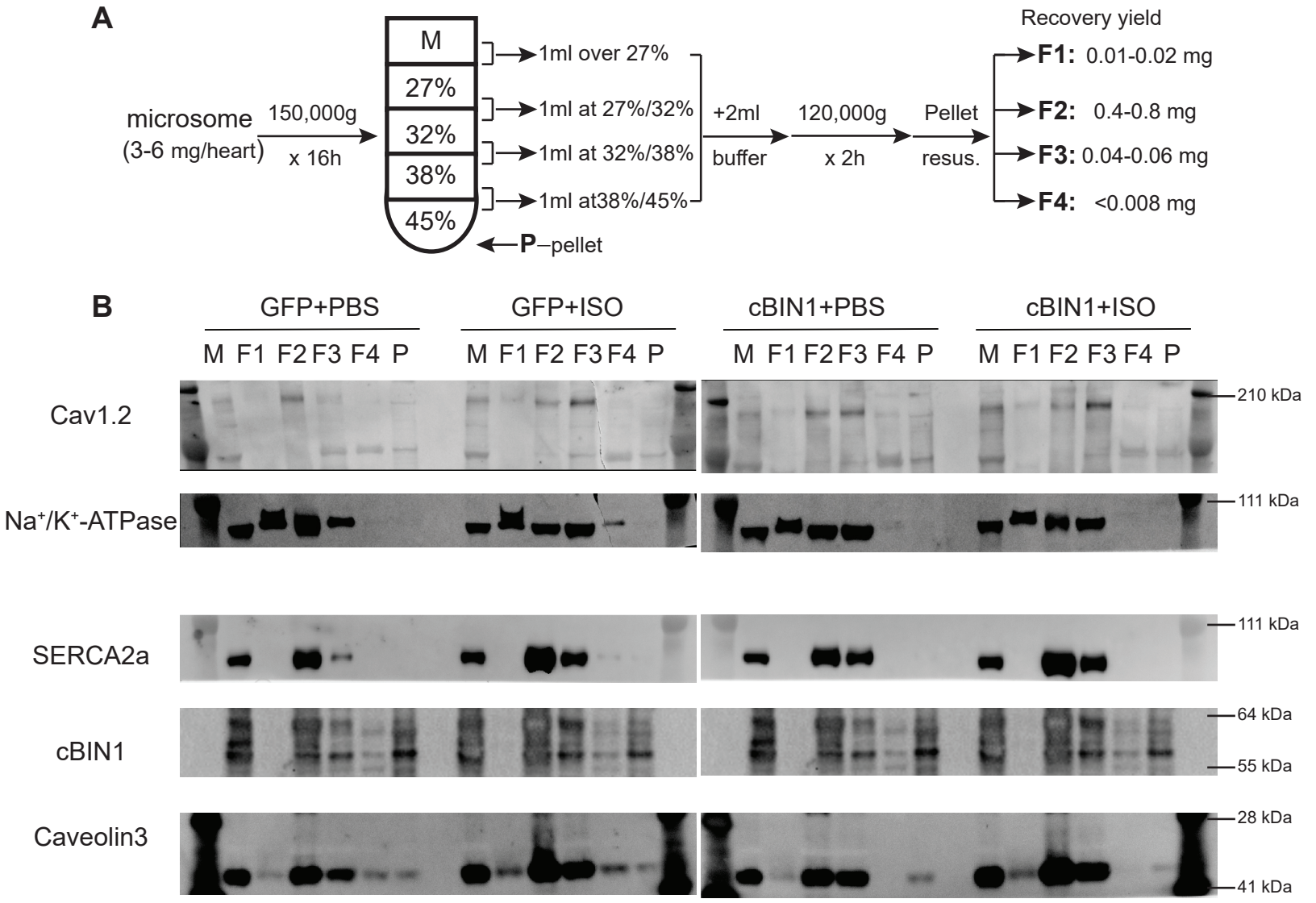

Supplemental Figure 5

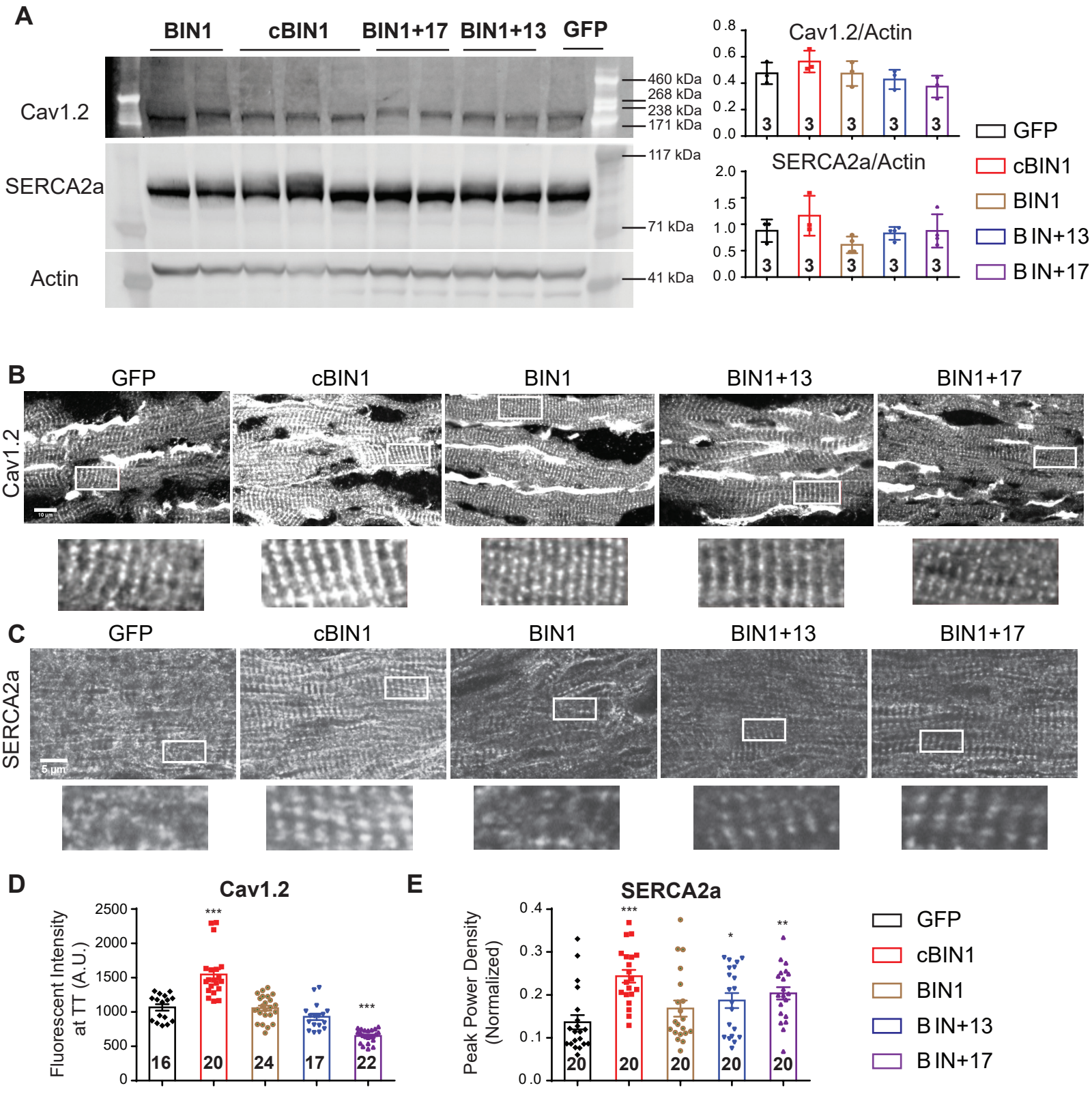

Supplemental Figure 6